

## Structural and thermodynamic properties of $C_x(BN)_{1-x}$ alloy

This article has been downloaded from IOPscience. Please scroll down to see the full text article.

1999 J. Phys.: Condens. Matter 11 3875

(<http://iopscience.iop.org/0953-8984/11/19/307>)

View [the table of contents for this issue](#), or go to the [journal homepage](#) for more

Download details:

IP Address: 171.66.16.214

The article was downloaded on 15/05/2010 at 11:32

Please note that [terms and conditions apply](#).

## Structural and thermodynamic properties of $C_x(BN)_{1-x}$ alloy

W Sekkal†, A Zaoui‡, A Laref†, H Aourag†§ and M Certier‡

† Computational Materials Science Laboratory, Physics Department, University of Sidi Bel-Abbes, 22000, Algeria

‡ LPLI 08 Rue Marconi, Technopôle 2000, 57078-Metz Cédex 3, France

E-mail: haourag@mail.univ-sba.dz

Received 7 December 1998, in final form 18 February 1999

**Abstract.** In this work, structural and thermodynamic properties of C–BN solid solutions are investigated using the well tested Tersoff potential. The bulk modulus is lower than those of diamond and cubic BN and the value predicted from considering ideal mixing between C and BN. Various thermodynamics quantities including the thermal expansion coefficient, heat capacity, Debye temperature and Grüneisen coefficient are also predicted.

### 1. Introduction

Carbon and boron nitride have similar crystalline structures: a layered hexagonal structure (h-BN) which is similar to that of graphite; the zinc-blende structure, analogous to that of diamond; and a rare hexagonal wurtzite structure (w-BN) corresponding to lonsdaleite [1–11]. They also have important physical characteristics in common. They share a number of similar physical properties including high melting temperatures ( $>3000$  K), large bulk moduli, high thermal conductivities and chemical inertness. Given the similarity in their phase diagrams and their atomic sizes, it is anticipated that a solid solution should exist across the carbon–boron nitride system at high pressure [12–14].

Synthesis of several samples across the cubic  $C_x(BN)_{1-x}$  solid-solution system ( $x = 0.3, 0.5, 0.6$ ) at pressures greater than 30 GPa and temperatures above 1500 K indicates that they are isostructural with diamond and cubic BN [15]. Such solid solutions may have physical properties similar to those of diamond and borazon, and are technologically very important.

Mixed C–BN layered hexagonal phases have been synthesized by a number of groups [16–18] and studied theoretically by Liu, Wentzcovitch and Cohen [19]. Badzian [16] has synthesized mixed crystals of diamond and c-BN by a high-temperature phase transformation technique. Other theoretical calculations are investigated using an empirical pseudopotential method [20] in order to study the electronic properties of  $C_x(BN)_{1-x}$ .

In this work, we study the crystal structure and calculate the structural and thermodynamic properties of  $C_x(BN)_{1-x}$  using a three-body potential which is well tested for diamond [21] and BN [22].

§ Author to whom any correspondence should be addressed. Fax: (213) 7 56 14 86.

## 2. Calculations

Among the many empirical model potentials that have been developed for tetrahedral semiconductors, that of Tersoff has been the most successful in that it reproduces many elemental-semiconductor properties, particularly those of silicon [23] and carbon [21]. Another form has been developed for multicomponent systems [24] to treat mixtures of these elements. The form of the energy  $E$ , between two neighbouring atoms  $i$  and  $j$ , is taken to be [24]

$$E = \sum_i E_i = \frac{1}{2} \sum_{i \neq j} V_{ij} \quad (1)$$

with

$$V_{ij} = f_C(r_{ij}) [a_{ij} f_R(r_{ij}) + b_{ij} f_A(r_{ij})] \quad (2)$$

where

$$f_R(r_{ij}) = A_{ij} \exp(-\lambda_{ij} r_{ij})$$

$$f_A(r_{ij}) = -B_{ij} \exp(-\mu_{ij} r_{ij})$$

$$f_C(r_{ij}) = \begin{cases} 1 & \text{for } r_{ij} < R_{ij} - D_{ij} \\ \frac{1}{2} - \frac{1}{2} \sin \left[ \frac{\pi}{2} \frac{(r_{ij} - R_{ij})}{D_{ij}} \right] & \text{for } R_{ij} - D_{ij} < r_{ij} < R_{ij} + D_{ij} \\ 0 & \text{for } r_{ij} > R_{ij} + D_{ij}. \end{cases}$$

$b_{ij}$  is the many-body order parameter describing how the bond-formation energy is affected by the local atomic arrangement due to the presence of other neighbouring atoms (the  $k$ -atoms). It is a many-body function of the positions of atoms  $i$ ,  $j$  and  $k$ . It has the form

$$b_{ij} = \chi_{ij} (1 + \beta_i^n \zeta_{ij}^{n_i})^{-1/2n_i} \quad (3)$$

with

$$\zeta_{ij} = \sum_{k (\neq i, j)} f_C(r_{ik}) g(\theta_{ijk}) \exp[\lambda_3^3 (r_{ij} - r_{ik})^3]$$

$$g(\theta_{ijk}) = 1 + \frac{c_i^2}{d_i^2} - \frac{c_i^2}{d_i^2 + (h_i - \cos \theta_{ijk})^2}$$

$$a_{ij} = (1 + \alpha^n \eta_{ij}^n)^{-1/2n_i}$$

$$\eta_{ij} = \sum_{k (\neq i, j)} f_C(r_{ik}) \exp[\lambda_3^3 (r_{ij} - r_{ik})^3]$$

$$\lambda_{ij} = \frac{(\lambda_i + \lambda_j)}{2} \quad (4)$$

$$\mu_{ij} = \frac{(\mu_i + \mu_j)}{2} \quad (5)$$

$$A_{ij} = (A_i A_j)^{1/2} \quad (6)$$

$$B_{ij} = (B_i B_j)^{1/2}. \quad (7)$$

$\zeta$  is called the effective coordination number and  $g(\theta_{ijk})$  is a function of the angle between  $r_{ij}$  and  $r_{ik}$  that has been fitted to stabilize the tetrahedral structure. We note that  $\lambda_3$  and  $\alpha$  are set equal to zero [25].

$\chi$  is a parameter which strengthens or weakens the heteropolar bonds, relative to the value obtained by simple interpolation.

Tersoff originally proposed his model by giving the parametrization for diamond [21]. Recently, adjusted Tersoff parameters for BN were proposed [22] based on the fact that boron nitride and carbon have important physical characteristic in common. From these values and using the above equations (namely (1)–(7)), we have calculated the potential parameters ( $A$ ,  $B$ ,  $\lambda$ ,  $\mu$ ,  $n$ ,  $h$ ,  $\beta$ ,  $c$ ,  $d$ ) for  $C_{0.5}(BN)_{0.5}$ . On the basis of the transferability of the Tersoff potential [22,26], all of the parameters for  $C_{0.3}(BN)_{0.7}$  and  $C_{0.6}(BN)_{0.4}$  have been kept constant except the cut-off  $R$  and  $\chi$  which are adjusted to ensure the stability of each structure. All of the parameters are listed in table 1.

**Table 1.** The adjusted Tersoff parameters for  $C_{0.3}BN_{0.7}$ ,  $C_{0.5}BN_{0.5}$  and  $C_{0.6}BN_{0.4}$ .

	$C_{0.3}BN_{0.7}$	$C_{0.5}BN_{0.5}$	$C_{0.6}BN_{0.4}$
$A$ (eV)	1393.6	1393.6	1393.6
$B$ (eV)	346.7	346.7	346.7
$\lambda$ ( $\text{\AA}^{-1}$ )	3.47795	3.47795	3.47795
$\mu$ ( $\text{\AA}^{-1}$ )	2.21595	2.21595	2.21595
$n$	0.72751	0.72751	0.72751
$h$	-0.57058	-0.57058	-0.57058
$\beta$	$1.5724 \times 10^{-7}$	$1.5724 \times 10^{-7}$	$1.5724 \times 10^{-7}$
$c$	38049	38049	38049
$d$	4.384	4.384	4.384
$R$ ( $\text{\AA}$ )	1.948	1.951	1.956
$D$ ( $\text{\AA}$ )	0.15	0.15	0.15
$\chi$	0.98855	0.99450	0.99778

Using Monte Carlo (MC) calculations, the interactions are described for different concentrations by the Tersoff potential. In our simulation, we assume that the system is treated as two components (C and BN). Indeed, BN is considered as an equivalent one-component system interacting with carbon. Initially, C and BN are always located at the nodes of a diamond network with interaction via the Tersoff potential. For a single particle of type  $S_i$  and at position  $r_i$ , we randomly choose a new status  $S'_i$  (which might be equal to  $S_i$ ) and a

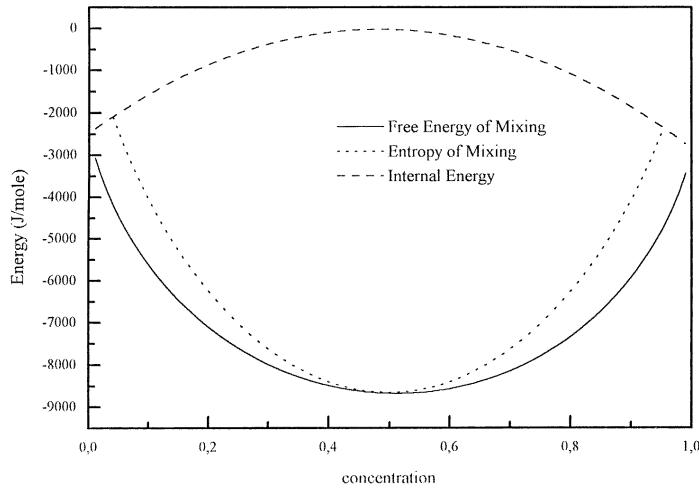


**Figure 1.** Free energy of mixing versus molar concentration for  $C_x(BN)_{1-x}$ .

slightly displaced new position  $r'_i$ , keeping the other particles and the box dimensions fixed. This random move is accepted or rejected by the usual Metropolis method (for more details, see reference [27]). So, although the nodes were moved stochastically, the topology of the lattice is fixed during the simulation.

On the basis of the above approximation, which considers the system as two components C and BN with the same size and shape, and with neglect of the freedom of orientation of the molecule BN, we calculate the entropy of mixing using the classical formula for a totally disordered solution:

$$S = R(x_C \ln(x_C) + x_{BN} \ln(x_{BN})) \quad (8)$$

where  $x$  is the molar concentration.

The internal energy of the system is a sum of interactions between pairs, C–C, BN–BN and C–BN. For the random case, the difference in internal energy between the alloy and the

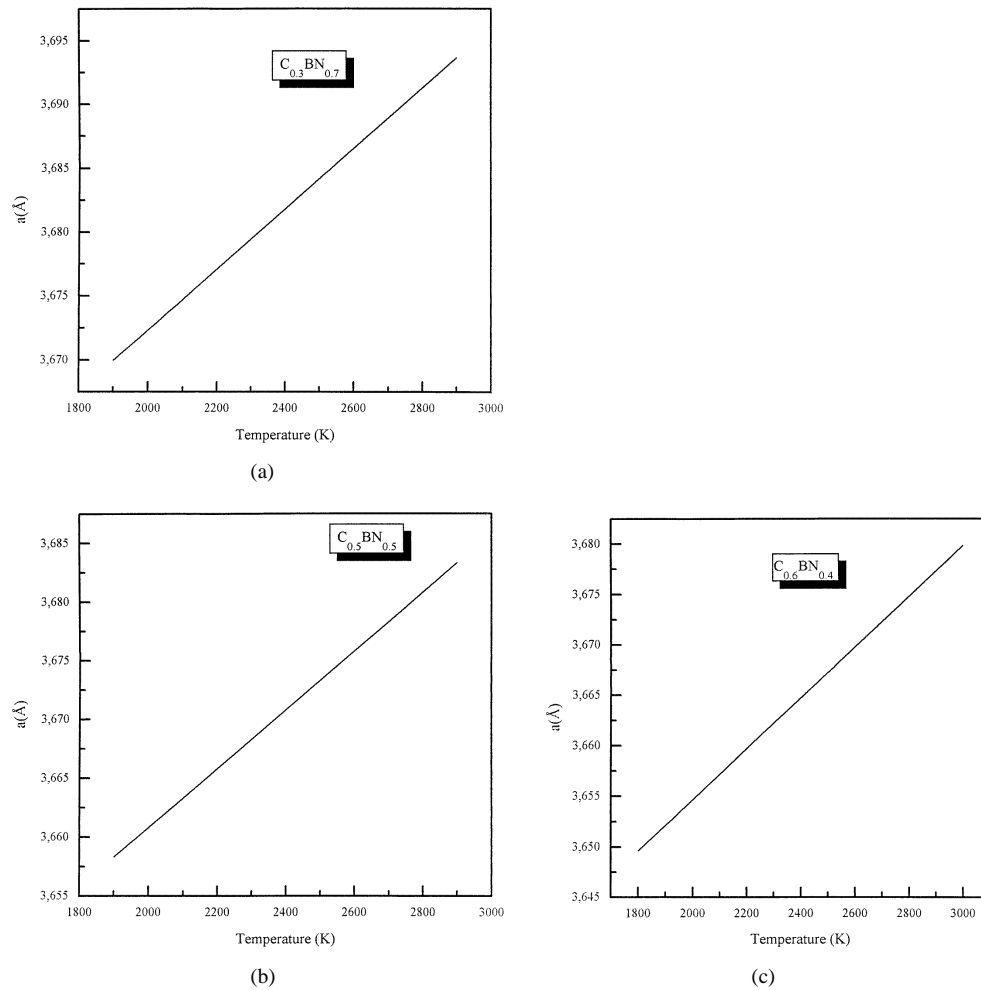


**Figure 2.** The lattice parameter as a function of temperature for  $C_{0.3}BN_{0.7}$  (a),  $C_{0.5}BN_{0.5}$  (b) and  $C_{0.6}BN_{0.4}$  (c).

mixture of pristine components can be written as

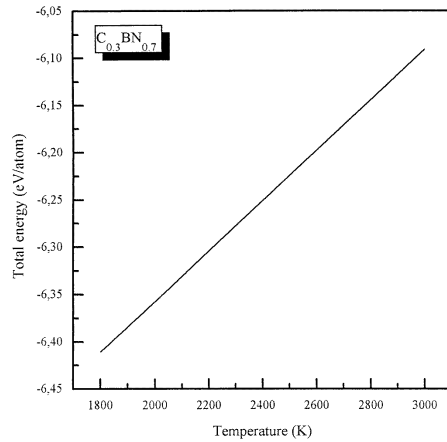
$$\Delta u = x_C x_C u_{C-C} \frac{Nz}{2} + x_{BN} x_{BN} u_{BN-BN} \frac{Nz}{2} + x_C x_{BN} u_{C-BN} Nz - x_C u_{C-C} \frac{Nz}{2} - x_{BN} u_{BN-BN} \frac{Nz}{2} \quad (9)$$

where  $z$  denotes the number of nearest neighbours,  $N$  the number of molecules in the system and  $u$  the intermolecular potential.

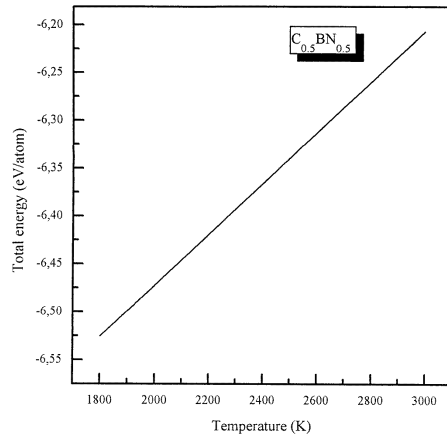
Using equations (8) and (9), the free energy of mixing is directly calculated. It is the difference between the energy and entropy terms:

$$F = \Delta u - TS. \quad (10)$$

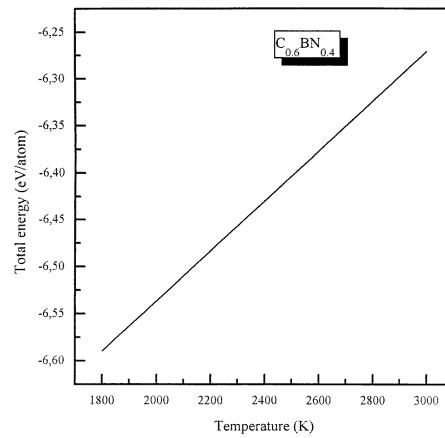
If C–BN solid solutions were stable at all concentrations, the free energy of mixing  $F$  for the system would be negative.



(a)



(b)



(c)

**Figure 3.** The total energy (per atom) of the system as a function of temperature for  $C_{0.3}BN_{0.7}$  (a),  $C_{0.5}BN_{0.5}$  (b) and  $C_{0.6}BN_{0.4}$  (c).

### 3. Results

We present in figure 1 the results of our calculations based on a MC method. As we see, the entropy is a symmetric function. This may be due to the approximation used in our calculations which considers C and BN as having the same size and shape. It appears that the entropic contribution to the free energy is responsible for the mixing effect. Indeed, the magnitude of the entropy term is larger, resulting in negative values for the Helmholtz energy of mixing. Consequently, C–BN solid solution can be considered stable at all concentrations.

X-ray diffraction studies [15] of the C–BN alloy at  $x = 0.3, 0.5$ , and  $0.6$  show that  $C_x(BN)_{1-x}$  is isostructural with diamond and BN. In order to obtain more information about the structural and thermodynamic properties of  $C_{0.3}BN_{0.7}$ ,  $C_{0.5}BN_{0.5}$  and  $C_{0.6}BN_{0.4}$  alloys, we ran a molecular-dynamics simulation using the Tersoff potential with 216 molecules. This system is allowed to relax into equilibrium by integrating the equations of motion through a

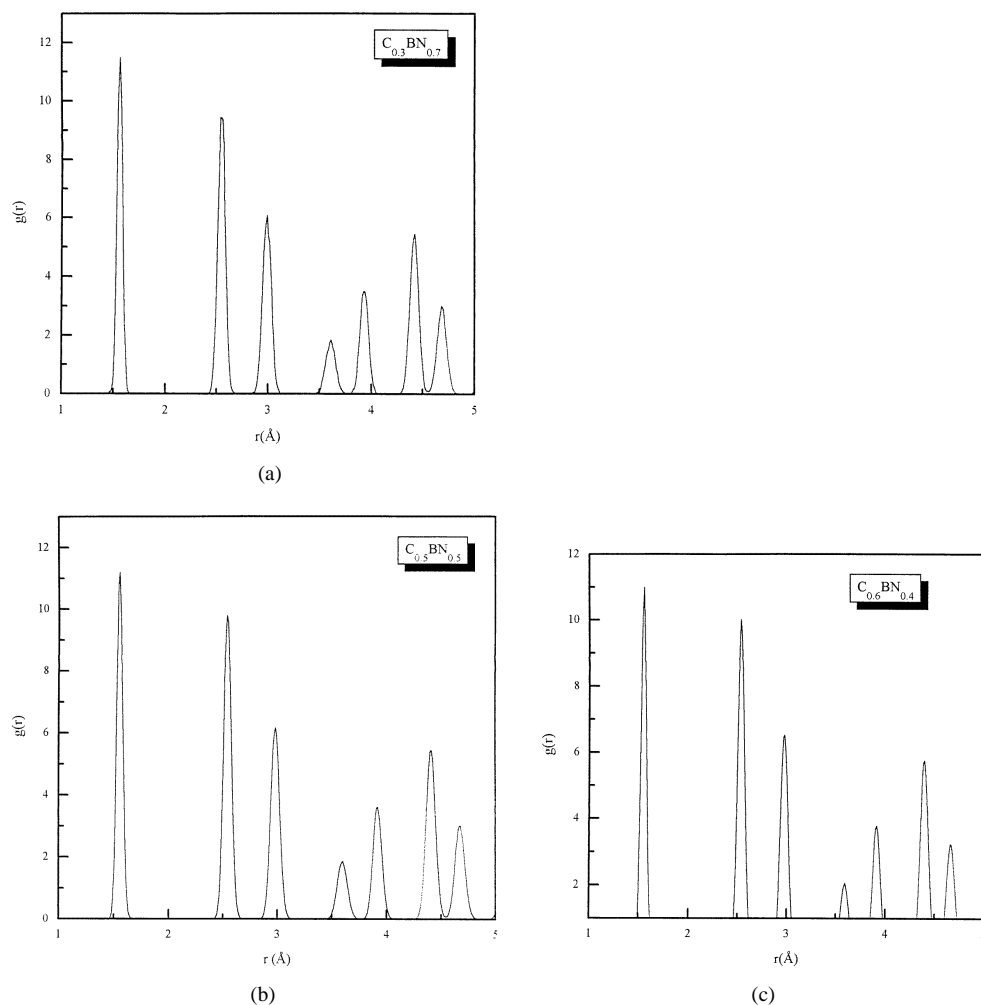


**Figure 4.** The pair correlation function for  $C_{0.3}BN_{0.7}$  (a),  $C_{0.5}BN_{0.5}$  (b) and  $C_{0.6}BN_{0.4}$  (c) at 300 K.

fifth-order Gear predictor–corrector algorithm with a time step  $h = 1.85$  fs. The simulation is carried out within the canonical  $NVT$ -ensemble where the temperature control is investigated using Andersen’s method [28]. After 40 ps, different properties are computed along the trajectory of the system in phase space.

The elastic constants ( $C_{11}$ ,  $C_{12}$  and  $C_{44}$ ) are determined using the method discussed in detail in reference [29]. From the elastic constants, we can predict the Debye temperature using the following empirical relation [30]:

$$\theta_D = -11.3964 + 0.3475C_{11} - 1.6150 \times 10^{-5}C_{11}^2. \quad (11)$$

In MD simulation, the linear thermal expansion coefficient  $\alpha_l$  can be computed directly from the definition

$$\alpha_l = \frac{1}{a} \left. \frac{\partial a}{\partial T} \right|_P \quad (12)$$

where  $a$  is the lattice parameter. Therefore, we consider the temperature variation of the lattice constant at zero pressure (see figures 2(a), 2(b), 2(c)). A molecular-dynamics simulation is performed in an  $NVT$ -ensemble at each temperature to equilibrate the system and then to determine the corresponding zero-pressure lattice constant. From the slope of the total-energy–temperature curve (see figures 3(a), 3(b), 3(c)), we can estimate the specific heat of the system according to the following equation:

$$C_v = \left| \left( \frac{\partial E}{\partial T} \right)_v \right|. \quad (13)$$

The Grüneisen constant can also be calculated using the following equation:

$$\gamma = \frac{3BV\alpha_l}{C_v} \quad (14)$$

where  $V$  is the molar volume.

Figures 4(a), 4(b), 4(c) display the pair distribution function  $g(r)$  for  $C_{0.3}BN_{0.7}$ ,  $C_{0.5}BN_{0.5}$  and  $C_{0.6}BN_{0.4}$  alloys. The results for the fourth peaks listed in table 2 are in good agreement with the experimental values of Knittle *et al* [15].

**Table 2.** Peak distances and numbers of pairs for  $C_{0.3}BN_{0.7}$ ,  $C_{0.5}BN_{0.5}$  and  $C_{0.6}BN_{0.4}$ .

Peak	$C_{0.3}BN_{0.7}$ distance (Å)	$C_{0.5}BN_{0.5}$ distance (Å)	$C_{0.6}BN_{0.4}$ distance (Å)	Number of pairs
First	1.560 <sup>a</sup> , 1.564 <sup>b</sup>	1.556 <sup>a</sup> , 1.559 <sup>b</sup>	1.542 <sup>a</sup> , 1.557 <sup>b</sup>	4.00 <sup>a</sup>
Second	2.536 <sup>a</sup> , 2.554 <sup>b</sup>	2.539 <sup>a</sup> , 2.546 <sup>b</sup>	2.536 <sup>a</sup> , 2.542 <sup>b</sup>	12.04 <sup>a</sup>
Third	2.991 <sup>a</sup> , 2.995 <sup>b</sup>	2.982 <sup>a</sup> , 2.986 <sup>b</sup>	2.966 <sup>a</sup> , 2.981 <sup>b</sup>	12.04 <sup>a</sup>
Fourth	3.609 <sup>a</sup> , 3.613 <sup>b</sup>	3.598 <sup>a</sup> , 3.602 <sup>b</sup>	3.592 <sup>a</sup> , 3.596 <sup>b</sup>	6.02 <sup>a</sup>

<sup>a</sup> Present work.

<sup>b</sup> Calculated from experimental results taken from reference [15].

Figures 5(a), 5(b), 5(c) display the cohesive energy versus volume for  $C_{0.3}BN_{0.7}$ ,  $C_{0.5}BN_{0.5}$  and  $C_{0.6}BN_{0.4}$  in the zinc-blende structure. The curves are fitted to Murnaghan’s equation of state [31] from which the equilibrium lattice parameter, the bulk modulus, its derivative and the cohesive energy are obtained. From the results listed in table 3, we notice the agreement of the lattice parameter and the bulk modulus for the zinc-blende structure with the experimental data [15]. The accuracy is around 0.02% for the lattice parameter and about 3% for the bulk modulus. The calculated bulk modulus is consistent with the relationship between the nearest-neighbour distance and bulk modulus for the diamond and zinc-blende structures [32].



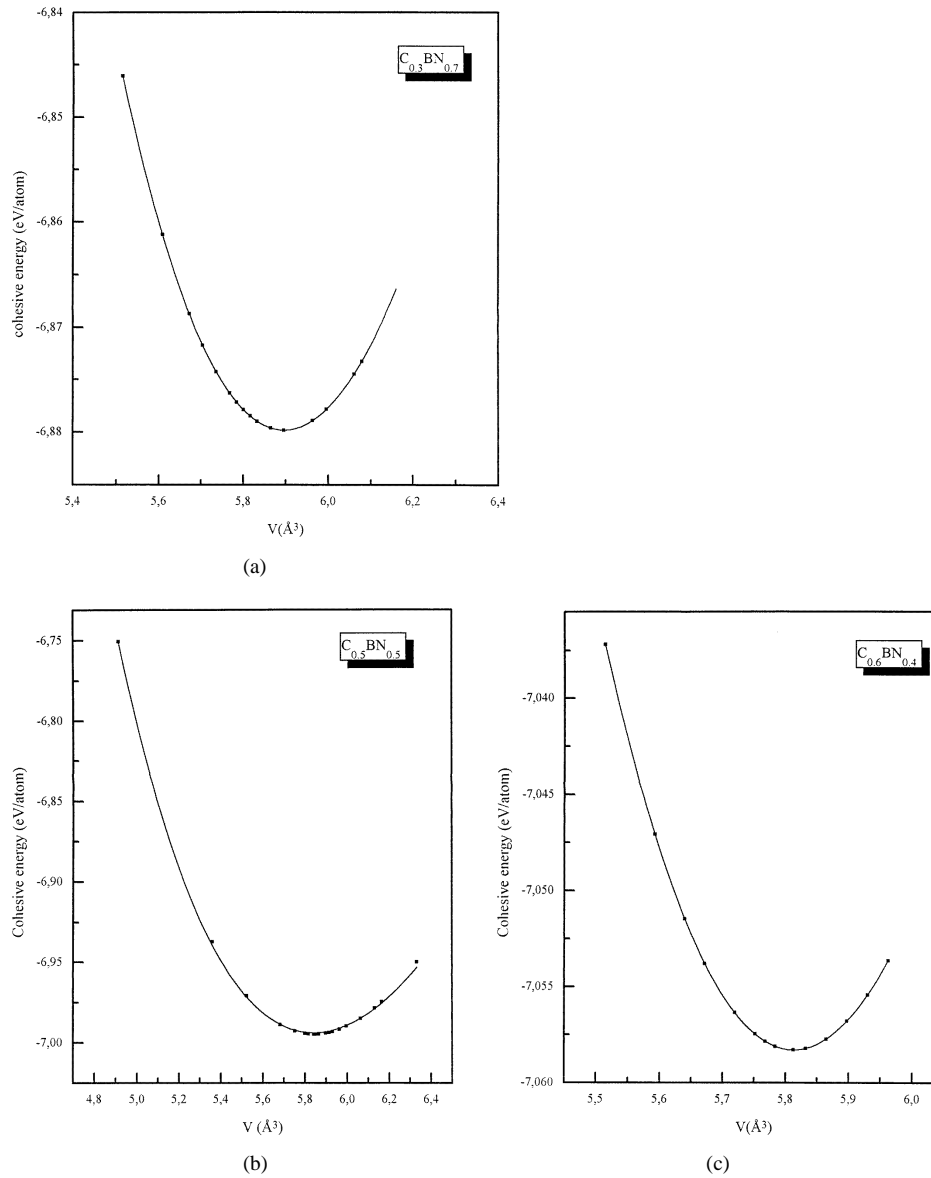


**Figure 5.** The cohesive energy of  $C_{0.3}BN_{0.7}$  (a),  $C_{0.5}BN_{0.5}$  (b) and  $C_{0.6}BN_{0.4}$  (c) versus molar volume.

Figures 6 and 7 show the nonideality of the lattice parameter and bulk modulus. The latter is smaller than the value predicted from its stoichiometry. However, the situation is reversed for the lattice parameter. The corresponding empirical relations are given respectively by the following relations:

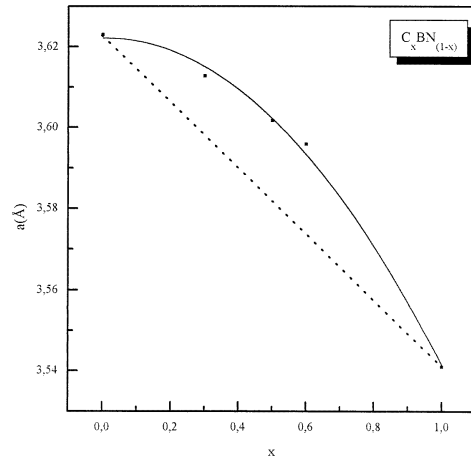
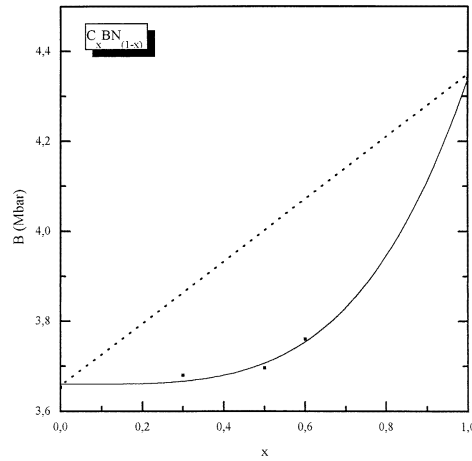
$$a \text{ (\AA)} = 3.62216 + 0.00085x - 0.08143x^2 \quad (15)$$

$$B \text{ (Mbar)} = 0.68x^{3.86} + 3.66. \quad (16)$$

The results for the elastic constants of C-BN are given in table 3 together with those of diamond

**Table 3.** Structural properties of  $C_{0.3}BN_{0.7}$ ,  $C_{0.5}BN_{0.5}$  and  $C_{0.6}BN_{0.4}$ .

	C	$C_{0.3}BN_{0.7}$	$C_{0.5}BN_{0.5}$	$C_{0.6}BN_{0.4}$	BN
$E_{coh}$ (eV/atom)	7.37 <sup>a</sup>	6.87 <sup>e</sup>	6.99 <sup>e</sup>	7.05 <sup>e</sup>	6.71 <sup>i</sup>
$a$ (Å)	3.567 <sup>a</sup>	3.612 <sup>e</sup> , 3.613 <sup>g</sup>	3.601 <sup>e</sup> , 3.602 <sup>g</sup>	3.595 <sup>e</sup> , 3.596 <sup>g</sup>	3.623 <sup>i</sup>
$B$ (Mbar)	4.43 <sup>b</sup>	3.68 <sup>e</sup> , 3.55 <sup>g</sup>	3.696 <sup>e</sup> , 3.699 <sup>h</sup>	3.76 <sup>e</sup> , 3.72 <sup>h</sup>	3.653 <sup>i</sup>
$B = (C_{11} + 2C_{12})/3$	4.46	3.68 <sup>e</sup>	3.695 <sup>e</sup>	3.757 <sup>e</sup>	
$B^{*f}$	4 <sup>c</sup>	6.5 <sup>e</sup>	4.95 <sup>e</sup>	7.7 <sup>e</sup>	3.94 <sup>i</sup>
$C_{11}$ (Mbar)	10.78 <sup>e</sup> , 10.80 <sup>d</sup>	9.32 <sup>e</sup>	9.51 <sup>e</sup>	9.63 <sup>e</sup>	9.9 <sup>j</sup>
$C_{12}$ (Mbar)	1.24 <sup>e</sup> , 1.3 <sup>d</sup>	0.86 <sup>e</sup>	0.79 <sup>e</sup>	0.82 <sup>e</sup>	4.41 <sup>j</sup>
$C_{44}$ (Mbar)	4.26 <sup>e</sup>	4.28 <sup>e</sup>	4.40 <sup>e</sup>	4.47 <sup>e</sup>	3.94 <sup>j</sup>
$\theta_D$	1860 <sup>f</sup>	1824 <sup>e</sup>	1834 <sup>e</sup>	1837 <sup>e</sup>	1730 <sup>k</sup>
$C_v$ ( $k_B$ )	2.97 ( $T = 18004$ K) <sup>f</sup>	3.019 <sup>e</sup>	3.021 <sup>e</sup>	3.081 <sup>e</sup>	5.53 <sup>k</sup>
$\gamma$		1.090 <sup>e</sup>	1.050 <sup>e</sup>	1.053 <sup>e</sup>	
$\alpha_l$ ( $10^{-5} K^{-1}$ )	1.5 <sup>f</sup>	0.70 <sup>e</sup>	0.67 <sup>e</sup>	0.68 <sup>e</sup>	1.15 <sup>k</sup>

<sup>a</sup> Reference [33].<sup>b</sup> Reference [34].<sup>c</sup> Reference [35].<sup>d</sup> Reference [21].<sup>e</sup> Present work.<sup>f</sup> Reference [36].<sup>g</sup> Reference [15].<sup>h</sup> Reference [32].<sup>i</sup> Reference [22].<sup>j</sup> Reference [37].<sup>k</sup> Reference [38].**Figure 6.** The lattice parameter versus concentration for C–BN. The dotted line represents ideal mixing (Vegard's law) between the end-member diamond and cubic BN, while the full curve is the fit to our solid-solution data.**Figure 7.** The bulk modulus versus concentration for C–BN. The dotted line is a prediction for ideal mixing according to Vegard's law.

and BN. To the best of our knowledge, no direct experimental and theoretical data have been available up to now. However, the bulk modulus obtained from the  $C_{ij}$ -coefficients is in good agreement with that found from the direct calculations presented above.

We can see that the values of the bulk modulus for  $C_{0.3}BN_{0.7}$ ,  $C_{0.5}BN_{0.5}$  and  $C_{0.6}BN_{0.4}$  are close to that of BN, which means that C–BN solid solution may have structural properties

similar to those of BN rather than carbon. A number of thermodynamic properties such as the Debye temperature  $\theta$ , the heat capacity  $C_v$ , the mode Grüneisen parameter  $\gamma$  and the linear thermal expansion coefficient  $\alpha_l$  are also predicted. According to our results, we see that the variation of the Debye temperature with concentration is linear, according to the following equation:

$$\theta = 1807.826 + 51.54 x. \quad (17)$$

The specific heat for  $C_{0.3}BN_{0.7}$ ,  $C_{0.5}BN_{0.5}$  and  $C_{0.6}BN_{0.4}$  alloys is  $3.02 k_B$  at high temperatures. This constant value corresponds to the classical Dulong–Petit result ( $3 k_B$ ), which is obtained at high temperatures for all solids.

#### 4. Conclusions

We have presented a simulation method for the calculation of the structural and elastic properties of C–BN alloy. The calculated lattice parameter, the bulk modulus, its derivative and the cohesive energy are in good agreement with available experimental data. Different thermodynamic properties such as the Debye temperature, heat capacity, mode Grüneisen parameter and linear thermal expansion coefficient are predicted. Further improvements can be made as regards the thermodynamic behaviour by taking into account the freedom of orientation of BN molecules.

#### References

- [1] Akashi T, Sawaoka A and Saito S 1978 *J. Am. Ceram. Soc.* **61** 245
- [2] Bundy F P and Wentorf R H 1963 *J. Chem. Phys.* **38** 1144
- [3] Coleburn N L and Forbes J W 1968 *J. Chem. Phys.* **48** 555
- [4] Corrigan F R and Bundy F P 1975 *J. Chem. Phys.* **63** 3812
- [5] DiCarli P S 1967 *Bull. Am. Phys. Soc.* **12** 1127
- [6] Gust W H and Young D A 1977 *Phys. Rev. B* **15** 5012
- [7] Onodera A, Miyazaki H and Fujimoto N 1981 *J. Chem. Phys.* **74** 5814
- [8] Sumiya H, Iseki T and Onodera A 1983 *Mater. Res. Bull.* **18** 1203
- [9] Wentorf R H 1957 *J. Chem. Phys.* **26** 956
- [10] Wentorf R H 1961 *J. Chem. Phys.* **34** 809
- [11] Yamaoka S, Shimomura O, Akaishi M, Kanda H, Nagashime T, Fukunaga O and Akimoto S 1986 *Physica B* **139+140** 668
- [12] Vries R C 1972 *Cubic Boron Nitride: A Handbook of Properties; GE Report N 72CRD178*
- [13] Meskimen H J and Andreatch P J 1972 *J. Appl. Phys.* **43** 2944
- [14] Knittle E, Wentzcovitch R M, Jeanloz R and Cohen M L 1989 *Nature* **337** 349
- [15] Knittle E, Kaner R B, Jeanloz R and Cohen M L 1995 *Phys. Rev. B* **51** 12 149
- [16] Badzian A R 1981 *Mater. Res. Bull.* **16** 1385
- [17] Kosolalapova Ya T, Makarenko B N, Serebryakova T I, Prilutskii E V, Khorpyakov O T and Chenysheva O I 1971 *Poroshk. Metall.* **1** 27
- [18] Kaner R B, Kouvetakis J, Warble C E, Sarriker M L and Barlett N 1987 *Mater. Res. Bull.* **22** 299
- [19] Liu A Y, Wentzcovitch R M and Cohen M L 1989 *Phys. Rev. B* **39** 1760
- [20] Zaoui A, Certier M, Ferhat M, Pagès O and Aourag H 1999 *Phys. Status Solidi b* **212** 307
- [21] Tersoff J 1988 *Phys. Rev. Lett.* **61** 2879
- [22] Sekkal W, Bouhafis B, Aourag H and Certier M 1998 *J. Phys.: Condens. Matter* **10** 4975
- [23] Tersoff J 1988 *Phys. Rev. B* **38** 9902
- [24] Tersoff J 1989 *Phys. Rev. B* **39** 5566
- [25] Tersoff J 1988 *Phys. Rev. B* **37** 6991
- [26] Sekkal W, Aourag H and Certier M 1998 *J. Phys. Chem. Solids* **59** 1293
- [27] Dünweg B and Landau D P 1993 *Phys. Rev. B* **48** 14 182
- [28] Andersen H C 1980 *J. Chem. Phys.* **72** 2384
- [29] Mehl M J 1993 *Phys. Rev. B* **47** 2493

- [30] Sekkal W, Aourag H and Certier M 1998 *Comput. Mater. Sci.* **9** 295
- [31] Murnaghan F D 1944 *Proc. Natl Acad. Sci. USA* **30** 5390
- [32] Cohen M L 1985 *Phys. Rev. B* **32** 7988
- [33] Donohue J 1974 *The Structure of Elements* (New York: Wiley)
- [34] McSkimin H J and Andreatch P Jr 1972 *J. Appl. Phys.* **43** 985
- [35] Gschneidner K A Jr 1964 *Solid State Physics* vol 16 (New York: Academic) p 275
- [36] Pierson H O (ed) 1993 *Handbook of Carbon, Graphite, Diamond and Fullerenes: Properties, Processing and Applications* (Noyes Publications)
- [37] Ferhat M, Zaoui A, Certier M and Aourag H 1998 *Physica B* **252** 229
- [38] Edgar J H (ed) 1994 *Properties of Group III Nitrides (Electronic Materials Information Service (EMIS) Datareviews Series)* (London: IEE)